ACADEMIC PRESS

Available online at www.sciencedirect.com

SCIENCE DIRECT®

Journal of Solid State Chemistry 171 (2003) 329–333

JOURNAL OF SOLID STATE CHEMISTRY

http://elsevier.com/locate/jssc

Microscopic analysis of insulating magnetism of $La_4Ba_2Cu_2O_{10}$ and $Nd_4Ba_2Cu_2O_{10}$

Wei Ku,* H. Rosner, W.E. Pickett, and R.T. Scalettar

Department of Physics, University of California, One Shields Avenue, Davis, CA 95616, USA

Received 4 June 2002; accepted 26 July 2002

Abstract

The rare-earth ions La and Nd evidently play a crucial role in the spin ordering of the Cu(2+) moments in $(RE)_4Ba_2Cu_2O_{10}$ (''RE422''), because La422 is a ferromagnetic (FM) insulator (a rare occurrence anyway) while Nd422 is antiferromagnetic (AF). Here we introduce explicit Wannier function (the ''spin orbital'') for the problem that illustrates the unusually strong effect of covalency and extends to (and beyond) the rare-earth ions. Material constants t, U, and (interatomic) J are calculated (not fitted) directly from the Wannier functions and show that the FM interatomic direct exchange can overwhelm the usual AF superexchange. Computationally, La422 is compressed to the volume of Nd422 to demonstrate that volume difference is not the determining factor; rather it is local ''chemistry'' on the rare-earth ion. This viewpoint is couched within a more general approach to the magnetic insulator problem.

1. Introduction

Since the first discovery of the exceptional insulating ferromagnetism of the ''brown phase'' $La_4Ba_2Cu_2O_{10}$ (La422) [1,2], the role of the rare-earth elements in this series of compounds has remained puzzling, as the same half-filled Cu-d orbital in isostructural $Nd_4Ba_2Cu_2O_{10}$ (Nd422) was found to align antiferromagnetically instead [3–5] at low temperature, as expected from the standard Hubbard-model that supposedly describes such CuO compounds quite well. Illustrating the microscopic origin of such dramatically different magnetic behavior poses a great challenge to our *quantitative* theoretical understanding of many-body interactions in real materials.

Up to now, there exist only few pioneering attempts to challenge this difficult problem. With elaborate perturbation on a multiband Hubbard-like model [6], it is suggested that destructive interference of hopping paths (between sixth- and eighth-order terms) may suppress z-axis antiferromagnetic (AF) coupling in La422 and give a small ferromagnetic (FM) coupling, in a very narrow parameter range, while the Goodenough process [7] between nearest neighbors produces the in-plane FM order. (More recently, the possible ''crude link'' to the ''flat-band ferromagnetism'' from the Hubbard-model was also pointed out [8].) However, this description is not very satisfactory: besides the problem of the narrow parameter range, the resulting strength of the FM coupling is too small to account for the experiments [1]. Furthermore, the assumption of FM coupling between the nearest neighbors in the plane is difficult to adapt to the AF order in Nd422 [5].

On the other hand, the more quantitative approach employing density functional theory (DFT) [9], by comparing total energy of different magnetic phases [10], not only suffers from the unknown quality of the approximate energy functional, but also hides all the microscopic details in a black box. Thus, a unified scheme that is able to account for both systems and allows simultaneous intuitive insight and qualitative realism of ab initio level is highly desired.

In this paper, we report results from implementing the first step of one such ambitious scheme. By representing the (reformulated) ab initio second-quantized Hamiltonian with localized energy-resolved Wannier states (WSs) [11–15], bare parameters t, U, and interatomic J are directly evaluated based on all-electron wave

*Corresponding author.
E-mail address: weiku@mailaps.org (W. Ku).

0022-4596/03/$ - see front matter © 2003 Elsevier Science (USA). All rights reserved.
doi:10.1016/S0022-4596(02)00212-8

functions. From these parameters, the key physical processes are easily illustrated: in La422, the strong intersite FM direct exchange [16], occurring at La sites, overwhelms the Hubbard-type AF superexchange [17], while in Nd422 the latter is strongly enhanced via the enormous increase in (001) hopping. This enhanced hopping is mediated by the additional channels via O sites, as clearly visualized from the spatial distribution of the half-filled WSs. Surprisingly, the in-plane order of both materials is found to be controlled by FM coupling between (101) neighbors, *not* coupling between the nearest neighbors, as currently assumed. The dramatic effect of the chemical environment is further demonstrated via calculation of La422 "under pressure", which not only illustrates the realistic "size effect", but also suggests an intriguing pressure-induced FM-to-AF phase transition upon higher pressure.

2. Theory

In order to faithfully reveal the microscopic detail, instead of the common approach of mapping the system onto a model Hamiltonian [15,18], we start with the full ab initio second-quantized Hamiltonian, *rigorously* reformulated into a "fluctuation" form that explicitly utilizes DFT solutions (without "double-counting" exchange-correlation effects) [19]

$$H = \varepsilon_{\bar{\mu}\alpha} n_{\bar{\mu}\alpha} - t_{\bar{\mu}\nu} c^{+}_{\bar{\mu}\alpha} c_{\bar{\nu}\alpha} + U_{\bar{\mu}} \tilde{n}_{\bar{\mu}\uparrow} \tilde{n}_{\bar{\mu}\downarrow} + \tfrac{1}{2} C_{\bar{\mu}\nu} \tilde{n}_{\bar{\mu}\alpha} \tilde{n}_{\bar{\nu}\beta} - J_{\bar{\mu}\nu} (S_{\bar{\mu}} \cdot S_{\bar{\nu}} + \tfrac{1}{4} n_{\bar{\mu}\alpha} n_{\bar{\nu}\beta}) + \text{other } \widetilde{c^{+}_{\bar{\mu}\nu}} \widetilde{c_{\bar{\mu}'\alpha}} \widetilde{c^{+}_{\bar{\nu}\beta}} \widetilde{c_{\bar{\nu}\beta}} \text{ terms} + \text{constant terms}, \quad (1)$$

where summation over barred variables is understood and $\tilde{o} \equiv o - \langle o \rangle^{\mathrm{DFT}}$ denotes fluctuation from expectation value of operator o within DFT. Notice that the "direct exchange" (the fifth term) that directly couples the spins is omitted in existing Hubbard-model-based analysis of these materials and turns out to play a crucial role.

Evaluation of "bare" parameters in Eq. (1) with traditional constrained DFT calculation [15,18] is difficult, if possible. Alternatively, energy-resolved WSs are explicitly constructed from all-electron DFT orbitals[1] and then employed to evaluate the bare parameters from their definitions [19]

$$\varepsilon_{\mu\alpha} \equiv \langle \mu | h^{\mathrm{DFT}} - v^{xc} | \mu \rangle - U_{\mu} \langle n_{\mu\alpha} \rangle^{\mathrm{DFT}},$$

$$t_{\mu\nu} \equiv -\langle \mu | h^{\mathrm{DFT}} - v^{xc} | \nu \rangle (1 - \delta_{\mu\nu}) + J_{\mu\nu} \langle c^{+}_{\nu\bar{\beta}} c_{\mu\bar{\beta}} \rangle^{\mathrm{DFT}} \sim -\langle \mu | h^{\mathrm{DFT}} | \nu \rangle (1 - \delta_{\mu\nu}),$$

$$U_{\mu} \equiv \langle \mu\mu | v | \mu\mu \rangle, \quad C_{\mu\nu} \equiv \langle \mu\nu | v | \mu\nu \rangle (1 - \delta_{\mu\nu})$$

and

$$J_{\mu\nu} \equiv \langle \mu\nu | v | \nu\mu \rangle (1 - \delta_{\mu\nu}),$$

where h^{DFT}, v^{xc}, v^{ext}, and v are the DFT Hamiltonian, Kohn-Sham exchange-correlation potential, external potential, and bare Coulomb interaction. Following the first step of procedure given in Ref. [12], WSs, $|Rm\rangle$, are constructed by projecting trial functions onto the *chosen* subspace of DFT eigenstates (details are given elsewhere [24]). Owing to the simple case of one half-filled WS per Cu site, the resulting WSs are practically maximally localized [12]. The hopping parameter $t_{\mu\nu}$ is directly evaluated via a simple transformation: $\langle Rm | k\bar{m}'' \rangle \varepsilon_{k\bar{m}''} \langle k\bar{m}'' | R'm' \rangle$ from DFT eigenvalues $\varepsilon_{km''}$, which is much more accurate and straightforward than the traditional tight-binding *fit* [25]. Since the resulting parameters correspond to the exactly same band structure as the DFT solution, this procedure can be regarded as a perfect "downfolding" [26]. Finally, the rest of the parameters are evaluated via careful 6D numerical integration [19],[2] instead of parametrized atomic Slater integrals [27].

Now, a full solution of a complicated multi-band many-body Hamiltonian like Eq. (1) is very challenging and will require further development in physical approximations and numerical algorithms. Here, we proceed by identifying two leading mechanisms in Eq. (1) that control the magnetic order of the system: Hubbard-type AF superexchange [17] and FM direct exchange [16]. Their strength can be estimated by summing over leading coupling paths the *phenomenological* formulae: $\mathscr{J}^{SX}_{\mu\nu} \sim -4t^2_{\mu\nu}/W_{\nu}$ and $\mathscr{J}^{DX}_{\mu\nu} \sim J_{\mu\nu}/2$, where $W_{\nu} \sim U_{\nu}/2$ approximately accounts for effects of onsite repulsion, competing off-site Coulomb repulsion, and the possible virtual processes involving states of higher energy (screening). Similar renormalization is also applied to the direct exchange, considering the intersite nature of $J_{\mu\nu}$.[3]

The employment of the WSs (or "molecular orbitals in crystal") [11–15] as basis is strongly physically motivated. Unlike atomic orbitals, WSs are fully aware of the crystal and local symmetry, including periodicity, and form an orthonormal complete set. Furthermore,

[1] The DFT wave functions are evaluated with a full-potential code [20]. The popular employment of pseudopotential is avoided in this work to avoid possible serious inaccuracy due to lack of nodes in DFT orbitals [21]. LDA [22] and LSDA + U [23] are employed for La422 and Nd422, respectively. The employment of LSDA + U for the latter case is to split the Nd-*f* states away from the Fermi energy. Parameters for LSDA + U (chosen to be 6.7 and 0.7 eV) are not crucial as long as the hybridization with Cu-*d* states of interest is removed.

[2] In this work, the 6D integrations [19] include only accurate contributions within spheres centered at each atomic site, which should account for more than 90% of the contributions.

[3] The argument, that contribution from on-site intra-orbital exchange to density–density interaction should only be weakly screened [28], does not apply to the case here.

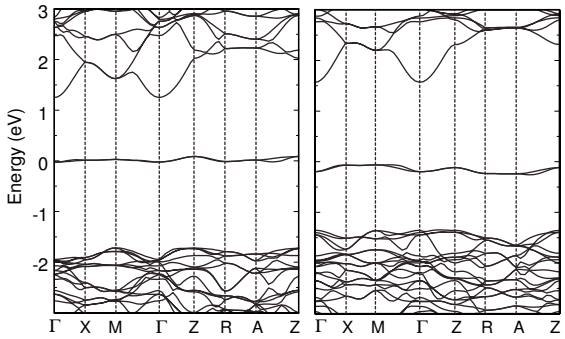

Fig. 1. Band structure of La422 (left panel) and Nd422 (right panel). Only the two narrow half-filled bands at Fermi level (0) possess spin moment.

nature of chemical bonding is automatically built into our WSs as will be shown in later discussion. Most importantly, our WSs are the *most localized within the subspace of low-energy excitation*, which naturally fit into the picture of localized spins interacting with each other. This energy resolution follows directly from the identity of subspace spanned by the WSs and the *chosen* DFT orbitals used to construct them. In addition, single-particle properties of the WSs (e.g.: "self-interaction" free [29] orbital energy, occupation number, and spin moment) can be directly translated from results of DFT calculation. Specifically for the problem of interest here, we are thus able to focus on only the two half-filled low-energy WSs, corresponding to the two partially occupied flat bands (Fig. 1), as other (particle or hole) states are of much higher energy and with zero spin moment. Also note that superexchange involving states of other higher energy states diminishes due to orthogonality between subspaces.

3. Discussion

The constructed half-filled low-energy WSs of La422, each centered at one Cu site, are illustrated in Fig. 2, in which isosurfaces of $|\langle x|Rm\rangle|^2$ in real space are plotted, along with the crystal structure. Note that the "hybridization" of Cu-*d*, O–*p*, and La-*d* orbitals is automatically built into the WSs; in traditional atomic-orbital approaches such effect would require inclusion of complicated "hopping", *t*, between several Cu, O, and La orbitals covering large energy range, which in turn obscure straightforward visualization of the dominant physical processes. The antibonding nature of Cu-*d* and O-*p* is also easily observed, as well as the fascinating "ring" structures at the La sites, which turn out to play an important role.

The spatial distribution of spin moment is reflected by that of the WSs, as $\langle x|\bar{R}\bar{m}\rangle\langle c^{+}_{\bar{R}\bar{m}\alpha}c_{\bar{R}'\bar{m}'\alpha}\rangle\langle\bar{R}'\bar{m}'|x\rangle \sim |\langle x|\bar{R}\bar{m}\rangle|^2\langle n_{\bar{R}\bar{m}\alpha}\rangle$. In our WS, only $\sim$50% of the spin moment resides at Cu sites, while each O possesses

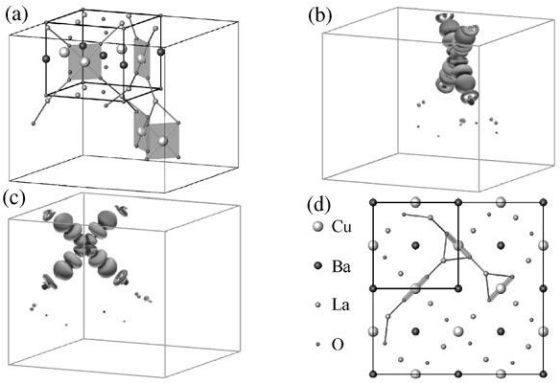

Fig. 2. Crystal structure of La422 (a) and its top view (d) shown within $2\times2\times2$ unit cells. Most atoms outside the first unit cell are removed in panel (a) for clarity. (b) and (c): Illustration of the low-energy WSs with $R=(0,0,0)$ [24].

Table 1
Calculated parameters for La422 (in meV). $U_i = 7.49$ eV

$j-i$	t_{ij}	J_{ij}
(001)	3.4	**1.3**
(111)	**3.6**	$\sim$0
(201)	**4.8**	$\sim$0
(021)	−0.10	$\sim$0
	$\left\|\mathcal{J}^{SX}_{z}\right\|$ −0.11	< $\left\|\mathcal{J}^{DX}_{z}\right\|$ 0.64

$j-i$	t_{ij}	J_{ij}
(101)	0.0	**1.1**
(100)	0.0	0.4
	$\left\|\mathcal{J}^{SX}_{x}\right\|$ −0.0	< $\left\|\mathcal{J}^{DX}_{x}\right\|$ 1.27

$j-i$	t_{ij}
(200)	**−8.8**
(020)	0.71
(210)	±0.84
(211)	±0.64

$\sim$10% of the moment. Intriguingly, small amount ($\sim$2%) of spin moment even extends to each La sites (Fig. 2), which naturally accounts for the unexpected large hyperfine field observed at La [2]. Our WSs also give, for the first time, detailed description of the shape of the local moment at La sites, as superposition of La-*d* orbitals, which NMR measurement have not been able to fully determine [2].

Let us first focus on the exceptional FM order in La422. The leading parameters of La422 are listed in Table 1, together with our estimated strength of AF superexchange and FM direct exchange. (Notice that the resulting U_i is much smaller than that of pure Cu-*d* orbital, reflecting the non-negligible spread of WSs to O-*p* orbitals.) Consistent with the extremely narrow bandwidth (Fig. 1), all the hopping parameters, t_{ij}, are very small, only a few meV. (i and j are labels of Cu sites, which form a cubic lattice with (100) being along the direction of Cu–O plaquette for the Cu in the origin.) Such weak hopping between sites brings about a weak AF trend via Hubbard-type superexchange along the *z*-axis (left panel). On the other hand, a much stronger *z*-axis FM coupling occurs through direct exchange that apparently overwhelms the AF superexchange. From Fig. 2, it is clear that such strong direct exchange occurs mainly via the ring structure of WSs at the La sites, where WSs overlap with each other along *z*-axis. This direct exchange process is similar to (but much

Table 2
Calculated parameters for Na422 (in meV). $U_I = 6.12$ eV

$j-i$	t_{ij}	J_{ij}
(001)	**−31**	2.1
(111)	**7.8**	∼0
(201)	**8.0**	∼0
(021)	−0.087	∼0
	$\left\|\mathcal{J}^{SX}_z\right\| = \left\|-1.71\right\| < \left\|\mathcal{J}^{DX}_z\right\| = \left\|1.06\right\|$	

$j-i$	t_{ij}	J_{ij}
(101)	0.0	**1.4**
(100)	0.0	1.1
	$\left\|\mathcal{J}^{SX}_x\right\| = \left\|-0.0\right\| < \left\|\mathcal{J}^{DX}_x\right\| = \left\|0.87\right\|$	

$j-i$	t_{ij}
(200)	−1.7
(020)	1.1
(210)	±1.4
(211)	±0.38

weaker than) what gives Hund's first rule in atoms. Note that the dominant direct exchange process has not been taken into account in existing Hubbard-model based microscopic analysis. From this, the difficulties of previous attempts are reasonably understandable.

Interestingly, the in-plane magnetic order of La422 is not dominated by coupling between nearest neighbors, as currently assumed. Instead, it is controlled by the (101) direct exchange that couples with second nearest neighbors above/below the nearest ones, as clearly shown in Table 1 (center panel). This FM exchange occurs mainly at the O sites, as easily observed in Fig. 2, and it is not challenged by superexchange due to zero hopping dictated by local symmetries. Our resulting coupling constants are of similar order of the observed transition temperature (∼5 K), which reinforces our phenomenological estimation.

Similar analysis is also applied to Nd422, as shown in Table 2.[4] The most striking feature is the tremendously enhanced z-axis hopping (left panel), which is ∼10 times larger than that of La422. A direct consequence is the greatly enhanced superexchange, which is now able to overcome the FM direct exchange, leading to the AF order along z-axis. This characteristic of 1D AF chain is in good agreement with optical and neutron measurement [3,5]. Intriguingly, the in-plane AF order is not controlled by the in-plane AF superexchange (center panel), which is forbidden by local symmetries as in the case of La. Instead, it is the (101) FM direct exchange that dominates the in-plane order between the 1D chains. (The competing (100) coupling is not only weaker, but also connected to fewer neighbors.)

Now turning attention to the origin of the dramatic difference between Nd422 and La422, we compare the half-filled WSs of both compounds in Fig. 3. Other than the change of spatial distribution of WSs near the Nd/La site, the key difference is the additional O-p structure in Nd422 at O sites that belong to the Cu one layer below/above. In addition to the moderate enhancement in the direct exchange, the main effect of this structure is to provide an alternative hopping channel. In atomic language, this extra Cu–O–O–Cu channel is much more

[4] Neutron diffraction measurement indicates that Nd-f moment is orthogonal to and "disconnected" from Cu-d moment [5] and is thus excluded from our analysis.

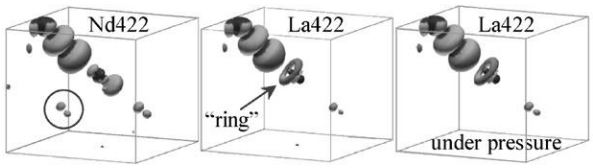

Fig. 3. Comparison of half-filled WSs of Nd422 (left), La422 (center), and La422 under pressure (right).

Table 3
Calculated parameters for La422 "under pressure." $U_i = 7.97$ eV

$j-i$	t_{ij}	J_{ij}
(001)	**−11.9**	**1.4**
(111)	**4.4**	∼0
(201)	**6.0**	∼0
(021)	−0.24	∼0
	$\left\|\mathcal{J}^{SX}_z\right\| = \left\|-0.29\right\| < \left\|\mathcal{J}^{DX}_z\right\| = \left\|0.69\right\|$	

$j-i$	t_{ij}	J_{ij}
(101)	0.0	1.2
(100)	0.0	0.3
	$\left\|\mathcal{J}^{SX}_x\right\| = \left\|-0.0\right\| < \left\|\mathcal{J}^{DX}_x\right\| = \left\|1.03\right\|$	

$j-i$	t_{ij}
(200)	**−10.3**
(020)	0.44
(210)	±0.69
(211)	±0.55

efficient than the Cu–O–La–O–Cu one. The difference in dominant hopping channels is clearly reflected in the different sign of (001) hopping of these two compounds, since t, unlike J, is sensitive to the relative phase of the WSs. In the case of La422, the hopping through O is much weaker, and only serves to slightly reduce hopping through La. This "interference" effect is similar to that discussed in Ref. [6], except that in our calculation, it is not responsible for the formation of ferromagnetism in La422.

To further investigate the driving force for the spatial redistribution (formation of O structure), results from another set of calculations of La422 are given in Fig. 3 and Table 3, in which lattice constants and atomic positions are set to those of Nd422. This third case corresponds approximately to La422 under pressure and allows us to distinguish the effect of interatomic distance vs. the "chemical" effect due to different chemical configurations.

From Fig. 3, it is apparent that the reduction of interatomic distance in the third case is not responsible for the spatial redistribution (no O-p in the right panel), even though it does slightly increase the degree of covalency as expected and observed from the small increase in (001) direct exchanges (left panel) in Table 3. The sign of the (001) hopping parameter further confirms the lack of hopping channel via O sites. We thus conclude that the key difference between La422 and Nd422 is the different chemical environment affected by La and Nd; the latter possesses 3 f-electrons and 3 more protons.

Intriguingly, even though the resulting magnetic order of the third case remains FM, in good agreement with the experimental observation of La422 under pressure [4], noticable enhancement (∼300%) in (001) hopping is observed due to enhanced covalency. This effect has evidently much stronger size dependence than the direct

exchange and thus suggests an unusual pressure-induced FM-to-AF transition upon higher pressure. We estimate that pressure slightly larger than 9 GPa will be able to trigger the transition. Alternatively, the transition should also be achievable via smaller pressure with $(La_{0.8}Nd_{0.2})_4Ba_2Cu_2O_{10}$.

4. Conclusion

With a newly developed theoretical scheme, the exceptional FM order observed in La422 is explained (by including direct exchange), as well as the AF order in isostructural Nd422. Detailed analysis shows that while La and Nd only possess small amount of the magnetic moment, the change of chemical environment does play a crucial role in determining the hopping channels and thus greatly affects the AF superexchange. The constructed WSs give valuable insight into the electron/spin interactions. While further development is desired, our approach already provides detailed and intuitive description of quantum magnetism, and thus complements the normal model approaches.

Acknowledgments

This work was supported by DOE Grant DE-FG03-01ER45876, ASCI through LLNL, and DAAD. Critical comment from R.R.P. Singh and discussion with A.K. McMahan and D.D. Koelling are acknowleged.

References

[1] F. Mizuno, et al., Nature 345 (1990) 28;
H. Masuda, et al., Phys. Rev. B 43 (1991) 7871.
[2] Pieper, et al., J. Magn. Magn. Mater. 135 (1994) 319.
[3] I.V. Paukov, et al., Phys. Lett. A 157 (1991) 306.
[4] H. Nozaki, et al., Phys. Rev. B 62 (2000) 9555.
[5] I.V. Golosovsky, et al., Phys. Lett. A 182 (1993) 161.
[6] S. Feldkemper, et al., Phys. Rev. B 52 (1995) 313.
[7] J.B. Goodenough, Phys. Chem. Solids 6 (1958) 287;
J. Kanamori, Phys. Chem. Solids 10 (1959) 87;
P.W. Anderson, Phys. Rev. 115 (1959) 2.
[8] H. Tasaki, Prog. Theor. Phys. 99 (1998) 489.
[9] W. Kohn, L.J. Sham, Phys. Rev. 140 (1965) A1133.
[10] V. Eyert, et al., Europhys. Lett. 31 (1995) 385; H. Rosner, Wei Ku, W.Pickett, R.T. Scalettar, to be published.
[11] G.H. Wannier, Phys. Rev. 52 (1937) 191.
[12] N. Marzari, D. Vanderbilt, Phys. Rev. B 56 (1997) 12847.
[13] V.P. Smirnov, D.E. Usvyat, Phys. Rev. B 64 (2001) 245108.
[14] G. Berghold, et al., Phys. Rev. B 61 (2000) 10040;
I. Schnell, et al., Phys. Rev. B 65 (2002) 075103.
[15] A.K. McMahan, et al., Phys. Rev. B 42 (1990) 6268.
[16] J.E. Hirsch, Phys. Rev. B 59 (1999) 436 and references therein.
[17] P.W. Anderson, Phys. Rev. 79 (1950) 350.
[18] M.S. Hybertsen, et al., Phys. Rev. B 39 (1989) 9028.
[19] Wei Ku, W.E. Pickett, R.T. Scalettar, to be published.
[20] P. Blaha, et al., WIEN2k, Technical University of Vienna, 2001.
[21] Wei Ku, A.G. Eguiluz, Phys. Rev. Lett. 89 (2002) 126401.
[22] J.P. Perdew, Y. Wang, Phys. Rev. B 45 (1992) 13244.
[23] V.I. Anisimov, et al., Phys. Rev. B 48 (1993) 16929;
A.I. Liechtenstein, et al., Phys. Rev. B 52 (1995) R5467.
[24] Wei Ku, H. Rosner, W.E. Pickett, R.T. Scalettar, Phys. Rev. Lett. 89 (2002) 167204.
[25] D.A. Papaconstantopoulos, M.J. Mehl, Phys. Rev. B 64 (2001) 172510 and reference therein.
[26] O.K. Andersen, et al., cond-mat/0203083.
[27] J.C. Slater, Quantum Theory of Atomic Structure, Vol. 1, McGraw-Hill, New York, 1960, p. 310.
[28] D. van der Marel, G.A. Sawatzky, Phys. Rev. B 37 (1988) 10674.
[29] J.P. Perdew, A. Zunger, Phys. Rev. B 23 (1981) 5048.